Phosphorylation-induced SUMOylation promotes Ulk4 condensation at ciliary tip to transduce Hedgehog signal

Mengmeng Zhou[1], Yuhong Han[1], and Jin Jiang[1,2,*]

[1]Department of Molecular Biology, University of Texas Southwestern Medical Center, Dallas, TX 75390, USA

[2]Department of Pharmacology, University of Texas Southwestern Medical Center, Dallas, TX 75390, USA

*Corresponding authors: jin.jiang@utsouthwestern.edu

Abstract

Hedgehog (Hh) signaling controls embryonic development and adult tissue homeostasis through the Gli family of transcription factors. In vertebrates, Hh signal transduction depends on the primary cilium where Gli is thought to be activated at the ciliary tip, but the underlying mechanism has remained poorly understood. Here we provide evidence that two Unc-51-like kinase (Ulk) family members Stk36 and Ulk4 regulate Gli2 ciliary tip localization and activation through phosphorylation and SUMOylation-mediated condensation in response to Shh. We find that Stk36-mediated phosphorylation of Ulk4 promotes its SUMOylation in response to Shh, and the subsequent interaction between SUMO and a SUMO-Interacting-Motif (SIM) in the C-terminal region of Ulk4 drives Ulk4 self-assembly to form biomolecular condensates that also recruit Stk36 and Gli2. SUMOylation or SIM-deficient Ulk4 failed to accumulate at ciliary tip to activate Gli2 whereas phospho-mimetic mutation of Ulk4 sufficed to drive Ulk4/Stk36/Gli2 condensation at ciliary tip, leading to constitutive Shh pathway activation in a manner dependent on Ulk4 SUMOylation. Taken together, our results suggest that phosphorylation-dependent SUMOylation of Ulk4 promotes kinase-substrate condensation at ciliary tip to transduce the Hh signal.

Introduction

The Hh family glycoproteins play essential roles in embryonic development and adult tissue homeostasis (Briscoe and Therond 2013; Jiang and Hui 2008). Aberrant Hh signaling contributes to a wide range of human diseases including birth defects and cancer (Jiang 2022; Nieuwenhuis and Hui 2005; Villavicencio, Walterhouse and Iannaccone 2000). Hh signaling in vertebrates critically depends on primary cilia (Goetz and Anderson 2010). In response to Hh stimulation, key Hh pathway components, including the GPCR family protein and Hh signal transducer Smoothened (Smo), as well as the pathway transcriptional factors Gli proteins, accumulate in primary cilia (Chen et al. 2009; Chen et al. 2011; Corbit et al. 2005; Haycraft et al. 2005; Rohatgi, Milenkovic and Scott 2007; Tukachinsky, Lopez and Salic 2010). Gli proteins are thought to be activated at the tip of primary cilia because Gli2 variants that fail to accumulate in the cilia cannot be activated both in cultured cells and in mouse embryos (Han et al. 2017; Liu, Zeng and Liu 2015; Santos and Reiter 2014); however, the underlying mechanisms that control ciliary tip localization and activation of Gli proteins have remained poorly understood.

Our previous studies showed that two Ulk family kinases, Ulk3 and Stk36, act in parallel to convert full-length Gli2 ($Gli2^F$) into its activator form ($Gli2^A$) by directly phosphorylating Gli2 at multiple sites in mammalian cells (Han et al. 2019; Zhou et al. 2022; Zhou and Jiang 2022). Another Ulk family member Ulk4, a pseudokinase, acts as a genetic modifier of the holoprosencephaly phenotype caused by impaired Shh pathway activity and physically interacts with Stk36 (Mecklenburg et al. 2021; Preuss et al. 2020). Our recent study demonstrated that Ulk4 acts in conjunction with Stk36 to

promote Gli2 phosphorylation and Hh pathway activation by forming a complex with Stk36 and regulating Stk36 ciliary accumulation (Zhou et al. 2023). Interestingly, we found that Stk36 and Ulk4 depend on each other for their ciliary localization and that ciliary tip localization of Ulk4 depends on Stk36-mediated phosphorylation of Ulk4 on T1021/T1023 (Zhou et al. 2023).

Here we provide evidence that phosphorylation of Ulk4 by Stk36 drives its phase separation to form biomolecular condensates that recruit Stk36, Gli2 and Sufu. We find that Stk36-mediated phosphorylation of Ulk4 at T1021/T1023 promotes its SUMOylation on an adjacent site (K1030) in response to Shh, and that interaction between SUMO and a SUMO-Interacting-Motif (SIM) in the C-terminal region of Ulk4 drives Ulk4 self-association to form biomolecular condensates. SUMOylation or SIM-deficient Ulk4 fails to accumulate at ciliary tip, thus unable to activate Gli2. Remarkably, a phospho-mimetic Ulk4 variant can form condensates that recruit Stk36, Gli2 and Sufu at ciliary tip in the absence of Shh, leading to constitutive Gli2 phosphorylation and pathway activation in a manner dependent on Ulk4 SUMOylation.

Results

Phosphorylation of Ulk4 is sufficient to drive its ciliary tip accumulation

Our previous study revealed that phosphorylation of Ulk4 by Stk36 is necessary for its ciliary tip accumulation (Zhou et al. 2023). To determine whether Ulk4 phosphorylation is sufficient to drive its ciliary tip accumulation, we generated a phospho-mimetic form of human Ulk4 (hUlk4) by converting two previously identified Stk36 sites (T1021 and

T1023) to E (Ulk4-EE). C-terminally HA-tagged wild type Ulk4 (Ulk4-WT) and Ulk4-EE were expressed in NIH3T3 cells via lentiviral infection, followed by Shh stimulation. As shown in Fig. 1A, Ulk4-WT-HA accumulated at ciliary tip only after Shh stimulation whereas Ulk4-EE-HA accumulated at ciliary tip regardless of Shh treatment. Quantification of ciliary tip Ulk4 signals revealed that Shh dramatically increased Ulk4-WT-HA levels but had little if any effect on Ulk4-EE-HA levels at ciliary tips (Fig. 1B), suggesting that Stk36-mediated phosphorylation of Ulk4 is sufficient to promote its ciliary tip accumulation.

We next asked whether Ulk4-EE could bring Stk36 to the ciliary tip in the absence of Shh. NIH3T3 cells were infected with lentivirus expressing Myc-tagged Stk36 (Myc-Stk36) and Ulk4-WT-HA or Ulk4-EE-HA, followed by immunostaining with antibodies against the epitope tags to monitor ciliary accumulation of Myc-Stk36 and Ulk4-WT-HA/Ulk4-EE-HA. Cells co-expressing Myc-Stk36 and Ulk4-WT-HA showed no ciliary tip accumulation of either Ulk4-WT-HA or Myc-Stk36 (Fig. 1C, D). By contrast, cells co-expressing Myc-Stk36 and Ulk4-EE-HA showed ciliary tip accumulation of both Ulk4-EE-HA and Myc-Stk36 (Fig. 1C, D), suggesting that Ulk4-EE could bring Stk36 to the ciliary tip even in the absence of Shh.

Gli2 ciliary tip accumulation is promoted by Stk36/Ulk4

In response to Shh, Gli proteins and their binding partner and Hh pathway inhibitor Sufu accumulate at ciliary tip while Smo accumulates along the cilium axoneme (Chen et al. 2009; Chen et al. 2011; Corbit et al. 2005; Haycraft et al. 2005; Rohatgi et al. 2007; Tukachinsky et al. 2010). The mechanisms that control ciliary tip localization of Gli

proteins are poorly understood although Kif7/Gli interaction has been implicated to play an important role (Haque et al. 2022). The observations that Stk36/Ulk4 colocalized with Gli2 at ciliary tip and that Ulk family kinases including Ulk3 and Stk36 acted upstream of Gli2 to promote Shh pathway activation let us to speculate that Gli ciliary tip localization could be regulated by these kinases. Indeed, as shown in Fig. 2A, B, Shh-induced ciliary accumulation of Gli2 and Sufu was diminished in Stk36 and Ulk3 double knockout (DKO) NIH3T3 cells (NIH3T3^{DKO}) (Han et al. 2019). Expression of wild type Stk36 (Stk36-WT) but not its kinase inactive form (Stk36-AA) restored ciliary tip accumulation of both Gli2 and Sufu in response to Shh (Fig. 2A, B). Furthermore, expression of Ulk4-EE but not Ulk4-WT in NIH3T3^{DKO} cells restored ciliary tip localization of both Gli2 and Sufu, which correlated with ciliary localization of Ulk4-EE (Fig. 2C-F). These results suggest ciliary tip localization of Glli2 and Sufu is promoted by Stk36 and Ulk4.

Phosphorylation drives Ulk4 condensation

The ciliary tip accumulation of Hh signaling components resembles biomolecular condensate formation that depends on multivalent interactions and protein concentrations (Banani et al. 2017; Shin and Brangwynne 2017). Indeed, Stk36, Ulk4, Gli and Sufu physically interact with one another (Han, Shi and Jiang 2015; Preuss et al. 2020; Zhou et al. 2023). Upon Hh stimulation, Smo is accumulated and activated in primary cilia, which may result in local activation of Stk36 kinase and Stk36-mediated phosphorylation of Ulk4, leading to their condensation that also recruits Gli2/Sufu. To test this hypothesis, we asked whether Stk36-mediated phosphorylation of Ulk4 can drive Stk36/Ulk4 condensation in the cytoplasm when both proteins were

overexpressed in HEK293T cells. Constitutively active Stk36 (Stk36-EE) or its kinase inactive form (Stk36-AA) was transfected into HEK293T cells together with Ulk4-WT. As shown in Fig. 3A, coexpression of Stk36-EE with Ulk4-WT led to the formation of Ulk4 puncta that also contained Stk36. However, coexpression of Stk36-AA with Ulk4-WT failed to induce the formation of Ulk4/Stk36 puncta. The formation of Ulk4/Stk36 puncta depends on phosphorylation of Ulk4 by Stk36 because HEK293T cells co-expressing a phospho-deficient form of Ulk4 (Ulk4-2TA) and Stk36-EE failed to form Ulk4/Stk36 puncta (Fig. 3B). Strikingly, HEK293T cells expressing Ulk4-EE formed Ulk4 condensates that also recruited endogenous Gli2 and Sufu into the condensates (Fig. 3C). These results suggest that phosphorylation of Ulk4 by Stk36 promotes the formation of Ulk4 condensates that can recruit its interaction proteins including Stk36, Gli2 and Sufu.

Most membraneless biomolecular condensates form through Liquid-Liquid phase separation (LLPS) that can be disrupted by 1, 6-hexanediol (McKnight 2024; Sabari et al. 2018). Indeed, the condensates of GFP-tagged YAP (GFP-YAP), which is formed via LLPS (Cai et al. 2019), were disrupted by treating cells with 5% 1, 6-hexanediol for 5 min (Fig. 3D). To determine the biomaterial property of the condensates organized by Ulk4, we treated HEK293T cells that contained CFP-Stk36/Ulk4-EE condensates with 5% 1, 6-hexanediol for 5 to 30 minutes. We found that CFP-Stk36/Ulk4-EE condensates were resistant to 1, 6-hexanediol even after treatment for 30 min (Fig. 3D; Fig. S1), suggesting that Stk36/Ulk4 condensates are more rigid than LLPS and may resemble gel-like or solid-state condensates (Putnam et al. 2019; Woodruff et al. 2017).

Shh induces SUMOylation of Ulk4 dependent on Stk36-mediated phosphorylation

We next asked how Ulk4 phosphorylation promotes its condensation. Phosphorylation can regulate other post-translational modifications (PTMs) such as SUMOylation, and SUMOylation has been implicated in the formation of biomolecular condensates (Keiten-Schmitz et al. 2021; Shen et al. 2006; Yang and Gregoire 2006). Interestingly, like Ulk4-mediated condensation, condensates formed by a synthetic construct containing multiple SUMO and SIM domains, RFP-SUMO6-SIM10 (Banani et al. 2016), were also resistant to 1, 6-hexanediol treatment (Fig. 3D; Fig. S1). Therefore, we asked whether phosphorylation induces Ulk4 condensation through promoting its SUMOylation. Coexpression of Ulk4-HA with Fg-Stk36-EE but not with Fg-Stk36-AA in HEK293T cells resulted in a mobility shift of Ulk4-HA indicative of SUMO conjugation (Fig. 4A, top panel). Probing with anti-SUMO1 antibody confirmed that higher molecular weight bands contained SUMOylated Ulk4 (Fig. 4A, bottom panel). Mutating the Stk36 sites on Ulk4 (Ulk4-2TA) abolished Ulk4 SUMOylation stimulated by Stk36-EE (Fig. 4B). On the other hand, Ulk4-EE was SUMOylated without coexpression of Stk36-EE, and SUMOylation of Ulk4-EE was abolished by a SUMOylation inhibitor TAK981 (Fig. 4C)(Langston et al. 2021). These results demonstrated that Stk36-mediated phosphorylation at T1021/T1023 can induce Ulk4 SUMOylation. Of note, SUMOylated Ulk4 tends to form high molecular weight species on the SDS-PAGE, a phenomenon also observed for SUMOylated nuclear hormone receptors (Poukka et al. 2000; Tian et al. 2002).

To determine whether Shh induces SUMOylation of Ulk4 dependent on its phosphorylation by Stk36, Ulk4-WT or Ulk4-2TA was expressed in NIH3T3 cells via

lentiviral infection, followed by Shh stimulation. As shown in Fig. 4D, Shh induced SUMOylation of Ulk4-WT but not Ulk4-2TA.

SUMOylation sites have consensus motifs: ψKxE/D or E/DxKψ, where ψ is a large hydrophobic amino acid and x could be any amino acid (Matic et al. 2010). SUMOylation of many proteins was promoted by phosphorylation on sites adjacent to the SUMOylation sites (Yang and Gregoire 2006). Inspection of Ulk4 C-terminal region identified a SUMOylation consensus site ($ESK_{1030}L$) adjacent to the Stk36 phosphorylation sites (Fig. 4E). To determine whether phosphorylation of Ulk4 at T1021/T1023 could promote SUMOylation at K1030, we carried out *in vitro* SUMOylation experiments. GST fusion proteins containing a Ulk4 fragment that encompasses both the Stk36 sites and the putative SUMOylation site (GST-Ulk4C; Fig. 4E) were incubated with immunopurified Stk36-EE and recombinant CK1 for *in vitro* phosphorylation, followed by incubation with SUMO1 and SUMO enzymes (E1 and E2) for *in vitro* SUMOylation. As shown in Fig. 4F, GST-Ulk4C was SUMOylated after kinase phosphorylation. Of note, CK1 was included to boost Stk36 kinase activity in the *in vitro* phosphorylation assay. Mutation of either K1030 to R (KR) or T1021/T1023 to A/A (2TA) abolished *in vitro* SUMOylation of GST-Ulk4C (Fig. 4F). Furthermore, the K1030R mutation abolished Stk36-induced SUMOylation of Ulk4 and the constitutive SUMOylation of Ulk4-EE (Ulk4-EE-KR) in HEK293T cells, as well as Shh-induced Ulk4 SUMOylation in NIH3T3 cells (Fig. 4G-I). Taken together, these results demonstrate that Shh induces SUMOylation of Ulk4 on K1030 dependent on its phosphorylation at T1021/T1023.

SUMOylation promotes Ulk4 self-association via SUMO/SIM interaction

SUMOylation mediates protein-protein interaction by binding to SIM, which consists of a stretch of hydrophobic amino acids adjacent to acidic residues (Song et al. 2004). Interestingly, Ulk4 contains a SIM motif ($_{1145}$EDLLLL$_{1151}$DLE) located C-terminally to phosphorylation-mediated SUMOylation site (Fig. 4E). To determine whether SUMOylation of Ulk4 promotes its self-association through interacting with SIM, we examined the interaction between Flag-tagged Ulk4-EE (Ulk4-EE-Fg), which is constitutively SUMOylated, or Ulk4-EE-KR-Fg, which is no longer SUMOylated (Fig. 4H), with HA-tagged wild type (Ulk4-WT-HA) or SIM-deficient Ulk4 (Ulk4-ΔSIM-HA; Fig. 4E). These constructs were transfected into HEK293T cells, followed by co-immunoprecipitation (Co-IP) and western blot analysis. As shown in Fig. 4J, Ulk4-EE-Fg formed a complex with Ulk4-WT-HA, which was diminished when SIM was mutated in Ulk4-WT-HA (Ulk4-ΔSIM-HA) or the SUMOylation site was mutated in Ulk4-EE-Fg (Ulk4-EE-KR-Fg). We also generated a C-terminal fragment of Ulk4-EE from aa1004-aa1275 of (C272-EE-Fg). C272-EE-Fg formed a complex with Ulk4-WT-HA albeit at lower affinity compared with Ulk4-EE-Fg; however, C272-EE-Fg failed to form a complex with Ulk4-ΔSIM-HA (Fig. 4K). These observations suggest that 1) SUMO-SIM interaction facilitates Ulk4 self-association through its C-terminal region and 2) the N-terminal region of Ulk4 can also mediate Ulk4 self-association independent of SUMO-SIM interaction.

SUMOylation and SIM are essential for Ulk4 condensation and Ulk4-mediated Shh pathway activation

To determine whether SUMOylation and SIM mediates Ulk4 condensation as is the case for PLM bodies (Shen et al. 2006), we coexpressed Stk36-EE with wild type (Ulk4-WT), SUMOylation deficient (Ulk4-KR), or SIM mutated Ulk4 (Ulk4-ΔSIM) in HEK293T cells. As shown in Fig. 5A, while Ulk4-WT formed condensates that contained Stk36-EE, neither Ulk4-KR nor Ulk4-ΔSIM formed condensates but rather exhibited diffused distribution in HEK293T cells.

Next, we expressed human Ulk4-WT, Ulk4-KR, or Ulk4-ΔSIM via lentiviral infection in NIH3T3 cells with endogenous Ulk4 depleted by shRNA and treated the cells with or without Shh. In contrast to Ulk4-WT, which was accumulated at the ciliary tip after Shh treatment, neither Ulk4-KR nor Ulk4-ΔSIM accumulated at ciliary tip in response to Shh stimulation (Fig. 5B, C). While Ulk4-WT rescued Gli2 phosphorylation, *Ptch1* and *Gli1* expression induced by Shh in Ulk4 depleted cells, neither Ulk4-KR nor Ulk4-ΔSIM rescued Gli2 phosphorylation and Shh target gene expression (Fig. 5D-F). These results suggest that Shh-induced Ulk4 SUMOylation and subsequent SUMO-SIM interaction is essential for Ulk4 condensation at ciliary tip and its role in mediating Shh pathway activation.

Ulk4-EE exhibits constitutive pathway activity dependent on its SUMOylation

Ulk4-EE formed condensates in the cytoplasm when expressed in HEK293T cells and accumulated at the ciliary tips in NIH3T3 cells in the absence of Shh. Treating cells with the SUMOylation inhibitor TAK-981 abolished Ulk4 condensation and ciliary tip accumulation (Fig. 6A-C), suggesting that Ulk4-EE condensation and constitutive ciliary tip localization may depend on its SUMOylation. To determine whether Ulk4-EE

condensation and constitutive ciliary tip localization depend on its SUMOylation at K1030, we examined Ulk4-EE-KR-Fg in which K1030 was mutated to R. In contrast to Ulk4-EE-Fg, Ulk4-EE-KR-Fg neither formed condensates in HEK293T cells nor accumulated at ciliary tip when expressed in NIH3T3 cells (Fig. 6D-F).

Consistent with its constitutive ciliary tip accumulation and its ability to recruit Stk36 and Gli2/Sufu to the ciliary tip (Fig. 1A, C; Fig. 2C-F), Ulk4-EE also exhibited constitutive pathway activity as indicated by Gli2 phosphorylation and transcriptional activation of *Ptch1* and *Gli1* in the absence of Shh (Fig. 6G-L). Blocking the SUMOylation of Ulk4-EE with either TAK-981 treatment or the K1030R mutation inhibited its constitutive pathway activity (Fig. 6G-L). Knockdown of Stk36 attenuated Shh-independent activation of *Ptch1* and *Gli1* induced by Ulk4-EE (Fig. S2A, B), suggesting that the constitutive pathway activity of Ulk4-EE depends on Stk36. Indeed, Ulk4-EE could activate Stk36 as indicated by the phosphorylation of the activation loop in the Stk36 kinase domain (p158T/pS1590; Fig. S2C) even though Stk36 is normally activated by Shh independent of Ulk4 (Zhou et al. 2023). Taken together, these results suggest that phosphorylation-mediated SUMOylation and subsequent SUMO-SIM interaction drives Ulk4 condensation that recruits Stk36 and Gli2 at ciliary tip, which is essential for Ulk4's role in mediating Shh signal transduction.

Discussion

How Hh converts the latent Gli transcription factor into its activator form at ciliary tip has remained an enigma in the field. Our previous study revealed that Stk36/Ulk4 acts in parallel with Ulk3 to promote Gli2 phosphorylation and activation in a manner

dependent on ciliary tip localization of Stk36/Ulk4, and that Shh-induced ciliary tip accumulation of this kinase/pseudokinase pair depends on phosphorylation of Ulk4 by Stk36 (Zhou et al. 2023). Here we demonstrate that phosphorylation of Ulk4 induces its SUMOylation and that subsequent SUMO-SIM mediated protein-protein interaction promotes ciliary tip condensation of Ulk4 that also recruits Stk36 and Gli2-Sufu, leading to Gli2 phosphorylation and activation (Fig. 7). We further showed that Shh-induced SUMOylation of Ulk4 depended on Ulk4 phosphorylation at T1021/T1023 and that a phospho-mimetic Ulk4 variant (Ulk4-EE) formed condensates that recruited Stk36 and Gli2 in the absence of Shh, leading to constitutive pathway activation.

Biomolecular condensates have been implicated in many cellular processes in which they function to facilitate biochemical reactions by simultaneously concentrating substrates and enzymes in the same subcellular compartments (Banani et al. 2017; Shin and Brangwynne 2017; Su, Mehta and Zhang 2021). The formation of biomolecular condensates through phase separation is often constitutive or regulated in response to stress signals. Whether phase separation can be induced by extracellular signals such as morphogens has been largely underexplored. Here we showed that Shh induces the formation of Ulk4 condensates that recruit Stk36 and Gli2 at ciliary tip to facilitate Gli2 phosphorylation and activation, providing a mechanistic insight into how Shh activates Gli proteins at ciliary tip. The formation of Stk36-Ulk4-Gli2 condensates at ciliary tip in response to Shh stimulation is likely due to local activation of Stk36 kinase by activated Smo accumulated at primary cilia and relatively high concentration of Stk36, Ulk4, Gli2 and Sufu at ciliary tips. Indeed, overexpression of Ulk4-EE or Stk36-

EE/Ulk4 in HEK293T cells led to the formation of Stk36/Ulk4 condensates in the cytoplasm that could also recruit endogenous Gli2 and Sufu.

In most cases, the formation of membraneless biomolecular condensates is driven by liquid-liquid phase separation (LLPS) mediated through intrinsically disordered regions (IDRs)/low-complexity domains (LCDs) (Banani et al. 2017; Shin and Brangwynne 2017). Here we showed that phosphorylation-regulated SUMOylation of Ulk4 and subsequent SUMO-SIM interaction is responsible for Shh-induced Stk36/Ulk4/Gli2 condensation at ciliary tip, which provides a mechanism that links kinase-mediated signaling and biomolecular condensation. Because phosphorylation-induced SUMOylation motifs are present in many regulatory proteins (Yang and Gregoire 2006), and SUMOylation has been implicated as a mechanism for condensate formation (Keiten-Schmitz et al. 2021), we speculate that phase separation driven by phosphorylation-dependent SUMOylation could be generally utilized in other settings and may represent a more general mechanism for kinase-mediated signaling.

Unlike liquid-like condensates whose formation is mediated by IDRs/LCDs and can be disrupted by 1,6 Hexanediol (McKnight 2024; Sabari et al. 2018), Ulk4/Stk36/Gli2 condensates are resistant to 1,6 Hexanediol treatment (Fig. 3D; Fig. S1), thus may resemble gel-like or solid-state condensates (Putnam et al. 2019; Woodruff et al. 2017). Interestingly, SUMO/SIM-mediated condensation of a synthetic construct (RFP-SUMO6-SIM10) also formed gel-like/solid-state condensates because they were resistant to 1,6 Hexanediol treatment (Fig. 3D; Fig. S1). It would be interesting to determine whether other condensates mediated by SUMO-SIM interaction such as PLM also exhibit gel-like/solid-state property.

Although Shh-induced SUMOylation of Ulk4 and SUMO-SIM-mediated interaction are essential for the formation of Ulk4/Stk36/Gli2/Sufu condensates, other protein-protein interaction events could also be important for the ciliary tip accumulation of these intracellular Hh signaling components. Indeed, a recent study revealed that Kif7-Gli2 interaction is essential for their ciliary tip accumulation (Haque et al. 2022). In the future, it would be interesting to explore the functional relationship between Kif7 and the Ulk family kinases in the regulation of ciliary accumulation of Gli proteins.

Materials and methods

DNA constructs

Myc-Gli2 was described previously (Han et al. 2019). Myc-Stk36, Fg-Stk36-WT, Fg-Stk36-EE, Fg-Stk36-AA, Ulk4-WT-HA, Ulk4-AA-HA, GST-Ulk4C-WT, GST-Ulk4C-2TA were generated previously (Zhou et al. 2023). C-terminally 3XHA-tagged human Ulk4-EE, Ulk4-KR, Ulk4-ΔSIM and C-terminally 3XFg-tagged Ulk4-EE, Ulk4-EE-KR, Ulk4-C272-EE were subcloned into the *FUGW* vector between EcoRI and BamHI sites. All GST fusion proteins were subcloned into the *pGEX 4T-1* vector between EcoRI and XhoI sites. Ulk4C-KR, Ulk4-C272-EE, Ulk4-KR, Ulk4-ΔSIM, Ulk4-EE, Ulk4-EE-KR plasmids were constructed by PCR-mediated site-directed mutagenesis.

Cell culture, transfection, and Shh treatment

NIH3T3 cells (ATCC, CRL-1658) were cultured in Dulbecco's modified Eagle's medium (DMEM, Sigma) with10% bovine calf serum (BCS, Gibco) and 1% penicillin-streptomycin (Sigma). GenJet Plus *in vitro* DNA transfection kit was used for transfection experiments according to the manufacturer's instruction (SignaGen). HEK293T cells (ATCC, CRL-11268) were cultured in DMEM containing 10% fetal bovine serum (FBS, Gibco) and 1% penicillin-streptomycin. Transfection was performed using the PolyJet *in vitro* DNA transfection kit (SignaGen) according to the instruction. For Shh treatment, the NIH3T3 cells were cultured at 50%-confluent densities in plate or chamber slides for one day and starved in serum-free medium (0.5% BCS) for 12 hours to allow ciliation. The recombinant human Shh N-terminal fragment (1 ng/ml; R&D

Systems, #8908-SH-005) was then added to the same serum-free medium for 12 hours or overnight.

Immunostaining, immunoprecipitation, and western blotting analysis

Immunostaining and quantification were carried out as previously described (Han et al. 2019; Zhou et al. 2023). Images were captured using Zeiss LSM700 laser scanning microscope. Fluorescence signal intensities were measured in the respective channel by ImageJ. 20 cells were randomly picked for each experimental group to measure ciliary tip fluorescence signal intensities. For Co-IP experiments were carried out as previously described (Han et al. 2019; Zhou et al. 2023). Western blot was carried out using standard protocol as previously described (Han et al. 2019; Zhou et al. 2023). Antibodies used in this study were as follows: Mouse anti-Myc (Santa Cruz Biotechnology; 9E10), Mouse anti-Flag (Sigma; M2), Mouse anti-HA (Santa Cruz Biotechnology; F7), Mouse anti-acetylated Tubulin (Sigma; T7451; staining:1:1000), Rabbit anti-Myc (Abcam; ab9106; staining 1:2000), Rabbit anti-HA (AbCam; ab9110; staining 1:500), Rabbit anti-SUMO1 (4930, Cell Signaling), Rabbit anti-Sufu (Abcam;ab28083; staining 1:500). Goat anti-HA (NOVUS; NB600-362; 1:400), Goat anti-Gli2 (R&D system; AF3635; staining 1:1000), Rabbit anti-pGli2 (pS230/232) (Han et al. 2019; Zhou et al. 2023), and Rabbit anti-pStk36 (pT158/pS159) (Shi et al. 2011; Zhou et al. 2023)

SUMOylation Assay

Cell-based SUMOylation assay was carried out as previously described (Han and Jiang 2022; Ma et al. 2016). Briefly, cell pellets were lysed at 4 °C for 10 min with lysis buffer containing 20 mM Tris HCl pH 8.0, 150 mM NaCl, 5 mM EDTA, 1% IGPAL CA-630, 10% glycerol, 1 mM DTT, 20 mM NEM, 1X protease inhibitors cocktail, 1X phosSTOP phosphatase inhibitors. SDS was added into the lysates to a final concentration of 1% and the mixture was boiled 5 min. After 5-fold dilution with cool lysis buffer, the mixture was subjected to immunoprecipitation and western blot analysis.

In vitro SUMOylation experiments were performed using the SUMOylation Assay Kit (Abcam; ab139470) following manufacturer's instruction. Flag-tagged Stk36-EE was transiently expressed in HEK293T cells, purified with anti-Fg agarose (Sigma; A2220) and eluted with Flag peptide (Sigma; F4799). The GST and GST fusion proteins were purified with glutathione beads (GE; 17-0756-01) and the resulting agarose were subjective to phosphorylation by Stk36-EE/CK1 as previously described (Zhou et al. 2022). The products of *in vitro* kinase assays were used as the substrates for *in vitro* SUMOylation assays.

1,6 hexanediol treatment

Cultured HEK293T cells were transfected with GFP-Stk36 and Ulk4-EE-HA, GFP-YAP or RFP-SUMO6SIM10 DNA constructs. After 48 hours, cells were treated with 5% 1,6 hexanediol for 5-30 minutes. Images were taken before and after treatment.

Lentivirus production and infection

To package the lentivirus, Ulk4 shRNA vector or *FUGW* lentiviral constructs were co-transfected with packaging plasmids (PSPAX2 and PMDG2) into HEK293T cells using PolyJet. After 48 hours to 72 hours of incubation, the supernatant was transferred to a 15 mL centrifuge tube and centrifuged at 2500 RPM for 15 minutes. After filtered through a 0.45 mM filter, the supernatant was collected into a new sterile tube (Beckman; 344059) and centrifuged at 20,000 g for 2 hours. The sediment was re-suspended, aliquoted in small volume of 10% FBS culture medium and stored at -80°C for future use. For cell infection, lentiviruses were added to 70% confluent wild type NIH3T3 cells together with Polybrene (Sigma, Cat. No. H9268) for overnight to get stable NIH3T3 cell lines.

RNA interference

The mouse Ulk4 shRNA lentiviral vector was purchased from Sigma (Sigma; TRCN0000328268). The Non target shRNA Plasmid DNA (Sigma; SHC016) was used as a control. The target sequence of mouse Ulk4 shRNA is: CTGCGAAGATTATCGAGAATG. The sequences for Stk36 siRNA were: 5'-GGUAUACUGGCUUCAGAAA-3' (Cat# SASI_ Mm02 _00345637) and 5'-GCCUUAUGUGCUUUGCUGU-3' (Cat# SASI_Mm01_00167751). The sequences for negative control were: 5'-UUCUCCGAACGUGUCACG U-3'. The knockdown efficiency was validated via real-time PCR.

Quantitative RT-qPCR

Total RNA was extracted from 1 × 10^6 cells using the RNeasy Plus Mini Kit (Qiagen; 74134), and cDNA was synthesized with High-Capacity cDNA Reverse Transcription Kit (Applied Biosystems; 01279158) and qPCR was performed using Fast SYBR Green Master Mix (Applied Biosystems; 2608088) and a Bio-Rad CFX96 real-time PCR system (BIO-RAD; HSP9601). The RT-qPCR was performed in triplicate for each of three independent biological replicates. Quantification of mRNA levels was calculated using the comparative CT method. Primers: Gli1, 5'-GTGCACGTTTGAAGGCTGTC-3' and 5'-GAGTGGGTCCGATTCTGGTG-3'; Ptch1, 5'-GAAGCCACAGAAAACCCTGTC-3' and 5'-GCCGCAAGCCTTCTCTACG-3'; Ulk4, 5'- ATGCAGAGTGTGATTGCGTTG-3' and 5'- GAGTGGCAGTTTCTGTGAACA-3'; Stk36, 5'-CGCATCCTACACCGAGATATGA-3' and 5'- AAATCCAAAGTCACAGAGCTTGA-3'; GAPDH, 5'-GTGGTGAAGCAGGCATCTGA-3' and 5'-GCCATGTAGGCCATGAGGTC-3'.

Reference

Banani, S.F., H.O. Lee, A.A. Hyman, and M.K. Rosen. 2017. "Biomolecular condensates: organizers of cellular biochemistry." *Nat Rev Mol Cell Biol* 18(5):285-298.

Banani, S.F., A.M. Rice, W.B. Peeples, Y. Lin, S. Jain, R. Parker, and M.K. Rosen. 2016. "Compositional Control of Phase-Separated Cellular Bodies." *Cell* 166(3):651-663.

Briscoe, J.and P.P. Therond. 2013. "The mechanisms of Hedgehog signalling and its roles in development and disease." *Nat Rev Mol Cell Biol* 14(7):418-431.

Cai, D., D. Feliciano, P. Dong, E. Flores, M. Gruebele, N. Porat-Shliom, S. Sukenik, Z. Liu, and J. Lippincott-Schwartz. 2019. "Phase separation of YAP reorganizes genome topology for long-term YAP target gene expression." *Nat Cell Biol* 21(12):1578-1589.

Chen, M.H., C.W. Wilson, Y.J. Li, K.K. Law, C.S. Lu, R. Gacayan, X. Zhang, C.C. Hui, and P.T. Chuang. 2009. "Cilium-independent regulation of Gli protein function by Sufu in Hedgehog signaling is evolutionarily conserved." *Genes Dev* 23(16):1910-1928.

Chen, Y., N. Sasai, G. Ma, T. Yue, J. Jia, J. Briscoe, and J. Jiang. 2011. "Sonic Hedgehog dependent phosphorylation by CK1alpha and GRK2 is required for ciliary accumulation and activation of smoothened." *PLoS Biol* 9(6):e1001083.

Corbit, K.C., P. Aanstad, V. Singla, A.R. Norman, D.Y. Stainier, and J.F. Reiter. 2005. "Vertebrate Smoothened functions at the primary cilium." *Nature* 437(7061):1018-1021.

Goetz, S.C.and K.V. Anderson. 2010. "The primary cilium: a signalling centre during vertebrate development." *Nat Rev Genet* 11(5):331-344.

Han, Y.and J. Jiang. 2022. "Cell-Based Assays for Smoothened Ubiquitination and Sumoylation." *Methods Mol Biol* 2374:139-147.

Han, Y., Q. Shi, and J. Jiang. 2015. "Multisite interaction with Sufu regulates Ci/Gli activity through distinct mechanisms in Hh signal transduction." *Proc Natl Acad Sci U S A* 112(20):6383-6388.

Han, Y., B. Wang, Y.S. Cho, J. Zhu, J. Wu, Y. Chen, and J. Jiang. 2019. "Phosphorylation of Ci/Gli by Fused Family Kinases Promotes Hedgehog Signaling." *Dev Cell* 50(5):610-626 e614.

Han, Y., Y. Xiong, X. Shi, J. Wu, Y. Zhao, and J. Jiang. 2017. "Regulation of Gli ciliary localization and Hedgehog signaling by the PY-NLS/karyopherin-beta2 nuclear import system." *PLoS Biol* 15(8):e2002063.

Haque, F., C. Freniere, Q. Ye, N. Mani, E.M. Wilson-Kubalek, P.I. Ku, R.A. Milligan, and R. Subramanian. 2022. "Cytoskeletal regulation of a transcription factor by DNA mimicry via coiled-coil interactions." *Nat Cell Biol* 24(7):1088-1098.

Haycraft, C.J., B. Banizs, Y. Aydin-Son, Q. Zhang, E.J. Michaud, and B.K. Yoder. 2005. "Gli2 and gli3 localize to cilia and require the intraflagellar transport protein polaris for processing and function." *PLoS Genet* 1(4):e53.

Jiang, J. 2022. "Hedgehog signaling mechanism and role in cancer." *Seminars in cancer biology* 85:107-122.

Jiang, J.and C.C. Hui. 2008. "Hedgehog signaling in development and cancer." *Dev Cell* 15(6):801-812.

Keiten-Schmitz, J., L. Roder, E. Hornstein, M. Muller-McNicoll, and S. Muller. 2021. "SUMO: Glue or Solvent for Phase-Separated Ribonucleoprotein Complexes and Molecular Condensates?" *Front Mol Biosci* 8:673038.

Langston, S.P., S. Grossman, D. England, R. Afroze, N. Bence, D. Bowman, N. Bump, R. Chau, B.C. Chuang, C. Claiborne, L. Cohen, K. Connolly, M. Duffey, N. Durvasula, S. Freeze, M. Gallery, K. Galvin, J. Gaulin, R. Gershman, P. Greenspan, J. Grieves, J.P. Guo, N. Gulavita, S. Hailu, X.Y. He, K. Hoar, Y.B. Hu, Z.G. Hu, M. Ito, M.S. Kim, S.W. Lane, D. Lok, A. Lublinsky, W. Mallender, C. McIntyre, J. Minissale, H. Mizutani, M. Mizutani, N. Molchinova, K. Ono, A. Patil, M. Qian, J. Riceberg, V. Shindi, M.D. Sintchak, K.L. Song, T. Soucy, Y.N. Wang, H. Xu, X.F. Yang, A. Zawadzka, J. Zhang, and S.M. Pulukuri. 2021. "Discovery of TAK-981, a First-in-Class Inhibitor of SUMO-Activating Enzyme for the Treatment of Cancer." *Journal of medicinal chemistry* 64(5):2501-2520.

Liu, J., H. Zeng, and A. Liu. 2015. "The loss of Hh responsiveness by a non-ciliary Gli2 variant." *Development* 142(9):1651-1660.

Ma, G., S. Li, Y. Han, S. Li, T. Yue, B. Wang, and J. Jiang. 2016. "Regulation of Smoothened Trafficking and Hedgehog Signaling by the SUMO Pathway." *Dev Cell* 39(4):438-451.

Matic, I., J. Schimmel, I.A. Hendriks, M.A. van Santen, F. van de Rijke, H. van Dam, F. Gnad, M. Mann, and A.C. Vertegaal. 2010. "Site-specific identification of SUMO-2 targets in cells reveals an inverted SUMOylation motif and a hydrophobic cluster SUMOylation motif." *Mol Cell* 39(4):641-652.

McKnight, S.L. 2024. "Protein domains of low sequence complexity-dark matter of the proteome." *Genes Dev* 38(5-6):205-212.

Mecklenburg, N., I. Kowalczyk, F. Witte, J. Gorne, A. Laier, T.M. Mamo, H. Gonschior, M. Lehmann, M. Richter, A. Sporbert, B. Purfurst, N. Hubner, and A. Hammes. 2021. "Identification

of disease-relevant modulators of the SHH pathway in the developing brain." *Development* 148(17).

Nieuwenhuis, E.and C.C. Hui. 2005. "Hedgehog signaling and congenital malformations." *Clin Genet* 67(3):193-208.

Poukka, H., U. Karvonen, O.A. Janne, and J.J. Palvimo. 2000. "Covalent modification of the androgen receptor by small ubiquitin-like modifier 1 (SUMO-1)." *Proc Natl Acad Sci U S A* 97(26):14145-14150.

Preuss, F., D. Chatterjee, S. Mathea, S. Shrestha, J. St-Germain, M. Saha, N. Kannan, B. Raught, R. Rottapel, and S. Knapp. 2020. "Nucleotide Binding, Evolutionary Insights, and Interaction Partners of the Pseudokinase Unc-51-like Kinase 4." *Structure* 28(11):1184-1196 e1186.

Putnam, A., M. Cassani, J. Smith, and G. Seydoux. 2019. "A gel phase promotes condensation of liquid P granules in Caenorhabditis elegans embryos." *Nat Struct Mol Biol* 26(3):220-226.

Rohatgi, R., L. Milenkovic, and M.P. Scott. 2007. "Patched1 regulates hedgehog signaling at the primary cilium." *Science* 317(5836):372-376.

Sabari, B.R., A. Dall'Agnese, A. Boija, I.A. Klein, E.L. Coffey, K. Shrinivas, B.J. Abraham, N.M. Hannett, A.V. Zamudio, J.C. Manteiga, C.H. Li, Y.E. Guo, D.S. Day, J. Schuijers, E. Vasile, S. Malik, D. Hnisz, T.I. Lee, Cisse, II, R.G. Roeder, P.A. Sharp, A.K. Chakraborty, and R.A. Young. 2018. "Coactivator condensation at super-enhancers links phase separation and gene control." *Science* 361(6400).

Santos, N.and J.F. Reiter. 2014. "A central region of Gli2 regulates its localization to the primary cilium and transcriptional activity." *J Cell Sci* 127(Pt 7):1500-1510.

Shen, T.H., H.K. Lin, P.P. Scaglioni, T.M. Yung, and P.P. Pandolfi. 2006. "The mechanisms of PML-nuclear body formation." *Mol Cell* 24(3):331-339.

Shi, Q., S. Li, J. Jia, and J. Jiang. 2011. "The Hedgehog-induced Smoothened conformational switch assembles a signaling complex that activates Fused by promoting its dimerization and phosphorylation." *Development* 138(19):4219-4231.

Shin, Y.and C.P. Brangwynne. 2017. "Liquid phase condensation in cell physiology and disease." *Science* 357(6357).

Song, J., L.K. Durrin, T.A. Wilkinson, T.G. Krontiris, and Y. Chen. 2004. "Identification of a SUMO-binding motif that recognizes SUMO-modified proteins." *Proceedings of the National Academy of Sciences of the United States of America* 101(40):14373-14378.

Su, Q., S. Mehta, and J. Zhang. 2021. "Liquid-liquid phase separation: Orchestrating cell signaling through time and space." *Mol Cell* 81(20):4137-4146.

Tian, S., H. Poukka, J.J. Palvimo, and O.A. Janne. 2002. "Small ubiquitin-related modifier-1 (SUMO-1) modification of the glucocorticoid receptor." *Biochem J* 367(Pt 3):907-911.

Tukachinsky, H., L.V. Lopez, and A. Salic. 2010. "A mechanism for vertebrate Hedgehog signaling: recruitment to cilia and dissociation of SuFu-Gli protein complexes." *J Cell Biol* 191(2):415-428.

Villavicencio, E.H., D.O. Walterhouse, and P.M. Iannaccone. 2000. "The sonic hedgehog-patched-gli pathway in human development and disease." *Am J Hum Genet* 67(5):1047-1054.

Woodruff, J.B., B. Ferreira Gomes, P.O. Widlund, J. Mahamid, A. Honigmann, and A.A. Hyman. 2017. "The Centrosome Is a Selective Condensate that Nucleates Microtubules by Concentrating Tubulin." *Cell* 169(6):1066-1077 e1010.

Yang, X.J.and S. Gregoire. 2006. "A recurrent phospho-sumoyl switch in transcriptional repression and beyond." *Mol Cell* 23(6):779-786.

Zhou, M., Y. Han, and J. Jiang. 2023. "Ulk4 promotes Shh signaling by regulating Stk36 ciliary localization and Gli2 phosphorylation." *Elife* 12.

Zhou, M., Y. Han, B. Wang, Y.S. Cho, and J. Jiang. 2022. "Dose-dependent phosphorylation and activation of Hh pathway transcription factors." *Life Sci Alliance* 5(11).

Zhou, M.and J. Jiang. 2022. "Gli Phosphorylation Code in Hedgehog Signal Transduction." *Front Cell Dev Biol* 10:846927.

Acknowledgements

We thank Bing Wang and Yong Suk Cho for helps during performing the experiments. J. Jiang is a Eugene McDermott Endowed Scholar in Biomedical Science at the University of Texas Southwestern.

Funding

This work was supported by grants from the National Institute of General Medical Sciences (R35GM118063) and Welch Foundation (I-1603).

Author contributions

Conceptualization: MMZ, YHH, JJ

Methodology: MMZ, YHH

Investigation: MMZ, YHH

Visualization: MMZ, YHH

Funding acquisition: JJ

Project administration: JJ

Supervision: JJ

Writing – original draft: MMZ, YHH, JJ

Writing – review & editing: MMZ, YHH, JJ

Competing interests

The authors declare that they have no competing interests.

Data and materials availability

All data are available in the main text or the supplementary materials.

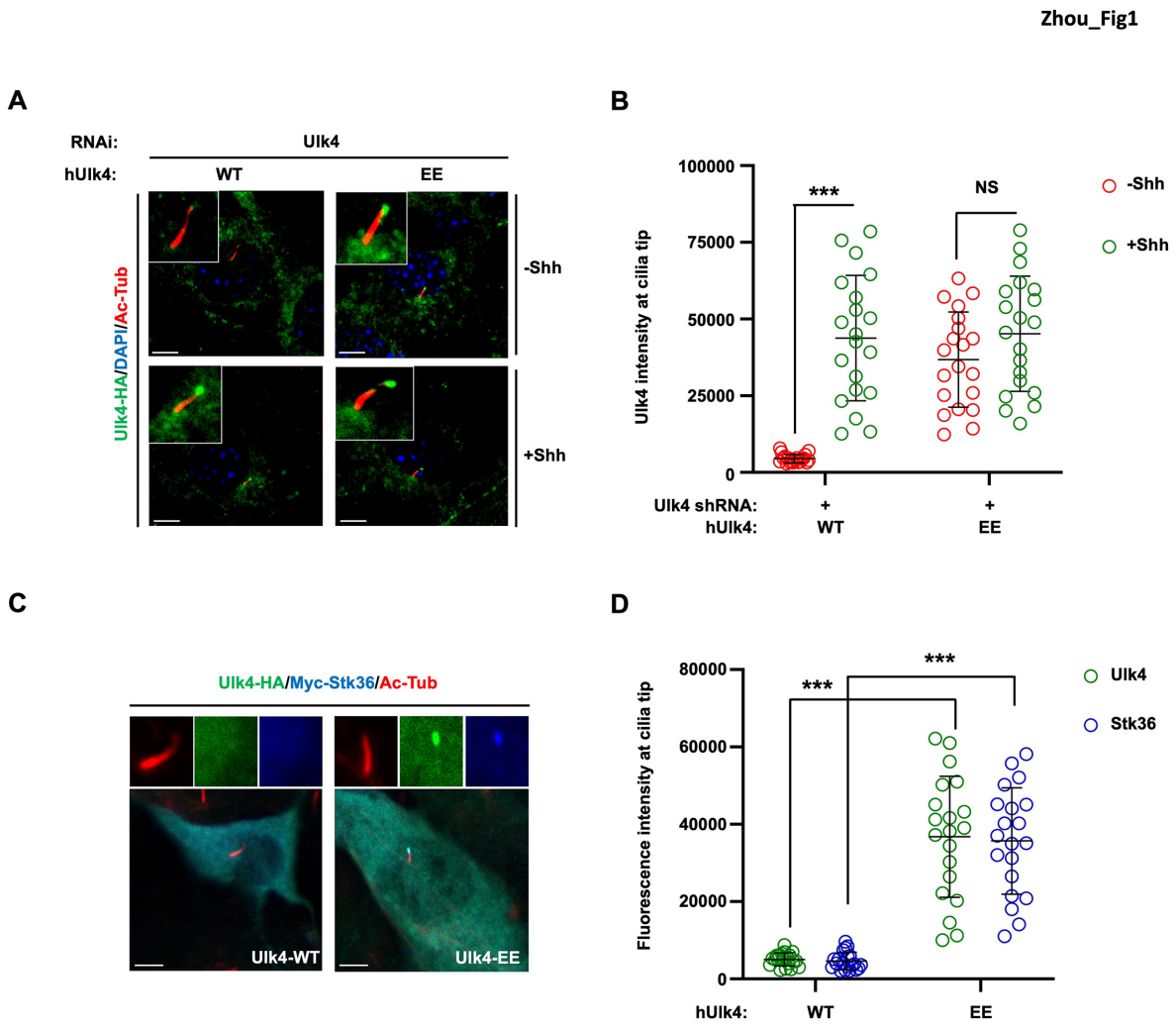

Fig. 1. Stk36-mediated phosphorylation of Ulk4 suffices to drive its ciliary tip accumulation

(A-B) Representative images of immunostaining (A) and quantification (B) of ciliary tip localized Ulk4-HA (green in A) in NIH3T3 cells infected with Ulk4 shRNA and lentivirus expressing human Ulk4-WT-HA or Ulk4-EE-HA in the presence or absence of Shh-N.

(C-D) Representative images of immunostaining (C) and quantification (D) of ciliary tip localized Ulk4-HA (green in C) or Myc-Stk36 (blue in C) in NIH3T3 cells infected with Ulk4-WT-HA or Ulk4-EE-HA lentivirus. Primary cilia were marked by acetylated tubulin (Ac-tub) staining (red in A and C). The intensity of ciliary-localized Ulk4-HA or Myc-Stk36 was measured by Image J. 20 cells were randomly selected from each experimental group for quantification. Data are mean ± SD from three independent experiments. ***$p < 0.001$ (Student's t test). Scale bars are 5 μm.

Zhou_Fig2

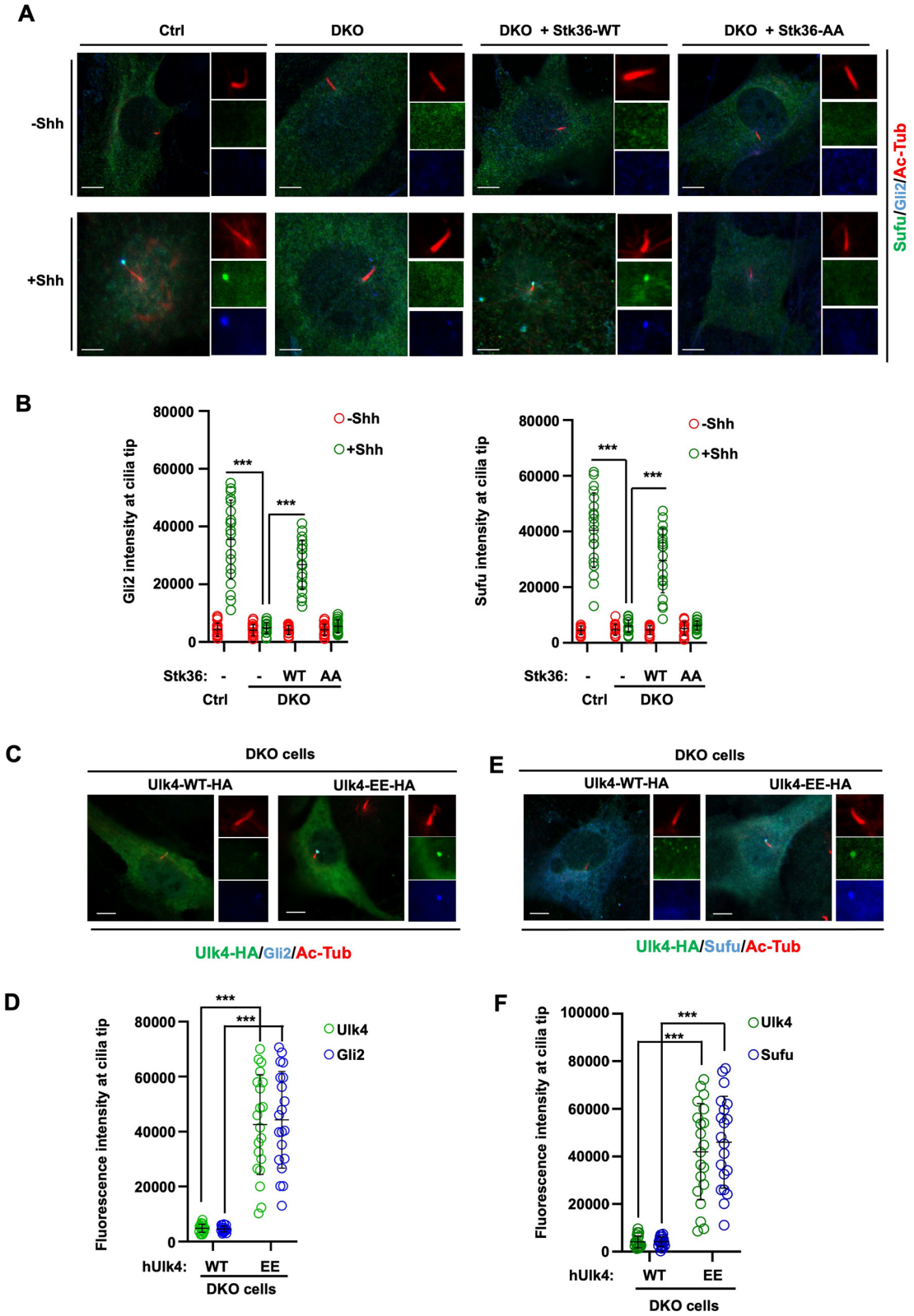
A
Ctrl
DKO
DKO + Stk36-WT
DKO + Stk36-AA
-Shh
+Shh
Sufu/Gli2/Ac-Tub
B
Gli2 intensity at cilia tip
Sufu intensity at cilia tip
-Shh
+Shh
***
Stk36: - - WT AA
Ctrl DKO
C
DKO cells
Ulk4-WT-HA
Ulk4-EE-HA
Ulk4-HA/Gli2/Ac-Tub
E
Ulk4-HA/Sufu/Ac-Tub
D
Fluorescence intensity at cilia tip
Ulk4
Gli2
hUlk4: WT EE
DKO cells
F
Sufu

Fig. 2. Stk36/Ulk4 promotes ciliary tip accumulation of Gli2 and Sufu

(A-B) Representative images of immunostaining (A) and quantification (B) of ciliary tip localized endogenous Sufu (green in A) or Gli2 (blue in A) in control or *Ulk3*^{KO} *Stk36*^{KO} (DKO) NIH3T3 cells infected with Stk36-WT or Stk36-AA lentivirus and treated with or without Shh-N.

(C-F) Representative images of immunostaining (C, E) and quantification (D, F) of ciliary tip localized Ulk4-HA (green in C, E), Gli2 (blue in C) or Sufu (blue in E) in DKO cells infected with Ulk4-WT-HA or Ulk4-EE-HA lentivirus.

Primary cilia were marked by acetylated tubulin (Ac-tub) staining (red in A, C and E). The intensity of ciliary-localized Sufu, Gli2 or Ulk4-HA was measured by Image J. 20 cells were randomly selected from each experimental group for quantification. Data are mean ± SD from three independent experiments. ***$p < 0.001$ (Student's t test). Scale bars are 5 μm.

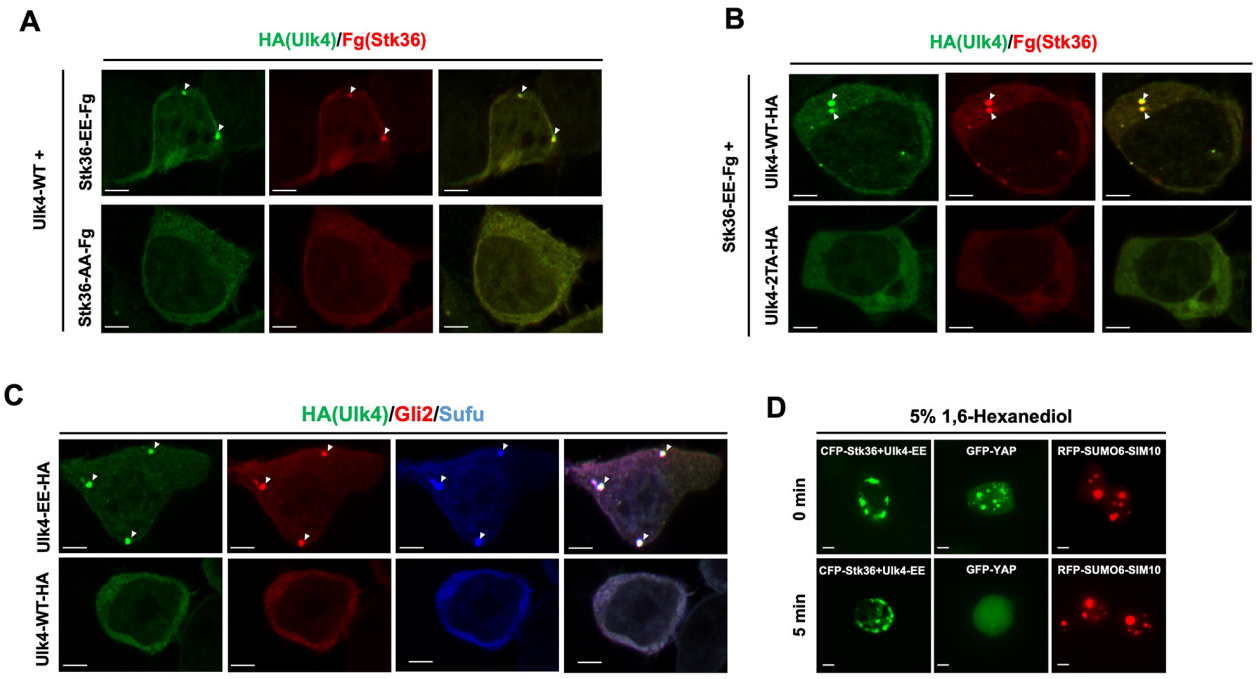

Fig. 3. Overexpression of phosphorylated Ulk4 drives its condensation outside primary cilia

(A-B) Representative images of immunostaining in HEK293T cells co-transfected with the indicated Ulk4-HA and Fg-Stk36 expression constructs. Arrowheads indicate Ulk4 (green in A and B) and Stk36 (red in A and B) puncta.

(C) Representative images of immunostaining in HEK293T cells transfected with Ulk4-EE-HA or Ulk4-AA-HA expression construct. Arrowheads indicate Ulk4-HA (green in C), Gli2 (red in C) or Sufu (blue in C) puncta.

(D) Representative images of HEK293T cells expressing the indicated constructs before and after treatment with 5% 1, 6-hexanediol for 5 minutes.

Scale bars are 6 μm.

Zhou_Fig4

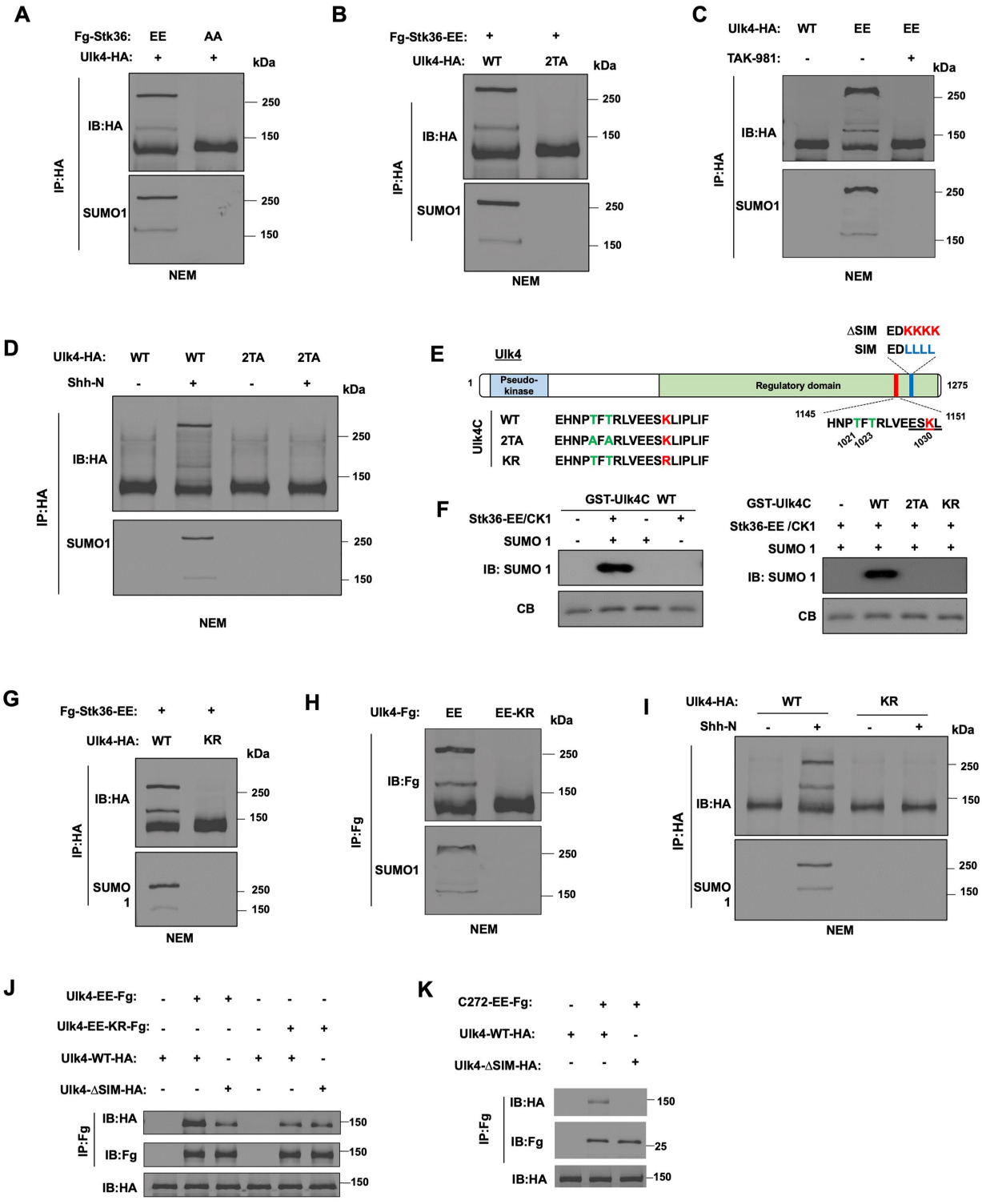
A
Fg-Stk36: EE AA
Ulk4-HA: + +
kDa
IB:HA
SUMO1
IP:HA
250
150
NEM
B
Fg-Stk36-EE: + +
Ulk4-HA: WT 2TA
C
Ulk4-HA: WT EE EE
TAK-981: - - +
D
Ulk4-HA: WT WT 2TA 2TA
Shh-N - + - +
E
Ulk4
Pseudo-kinase
Regulatory domain
1
1275
ΔSIM EDKKKK
SIM EDLLLL
1145
1151
HNPTFTRLVEESKL
1021 1023 1030
Ulk4C
WT EHNPTFTRLVEESKLIPLIF
2TA EHNPAFARLVEESKLIPLIF
KR EHNPTFTRLVEESRLIPLIF
F
GST-Ulk4C WT
Stk36-EE/CK1
SUMO 1
IB: SUMO 1
CB
GST-Ulk4C - WT 2TA KR
Stk36-EE /CK1
G
Fg-Stk36-EE: + +
Ulk4-HA: WT KR
H
Ulk4-Fg: EE EE-KR
IB:Fg
IP:Fg
I
Ulk4-HA: WT KR
Shh-N - + - +
J
Ulk4-EE-Fg: - + + - - -
Ulk4-EE-KR-Fg: - - - - + +
Ulk4-WT-HA: + + - + + -
Ulk4-ΔSIM-HA: - - + - - +
K
C272-EE-Fg: - + +
Ulk4-WT-HA: + + -
Ulk4-ΔSIM-HA: - - +
25

Fig. 4. Stk36-mediated phosphorylation promotes Ulk4 SUMOylation

(A-B) Western blot analysis of Ulk4 SUMOylation in HEK293T cells co-transfected with the indicated Fg-Stk36 and Ulk4-HA constructs. Cells were lysed in the presence of the deSUMOylation inhibitor NEM. Ulk4-HA was immunoprecipitated with anti-HA antibody, followed by western blot analysis with HA and SUMO1 antibodies.

(C) Western blot analysis of Ulk4 SUMOylation in HEK293T cells transfected with Ulk4-WT-HA or Ulk4-EE-HA construct and treated with or without TAK-981.

(D) Western blot analysis of Ulk4 SUMOylation in NIH3T3 cells infected with the indicated Ulk4 constructs and treated with or without Shh-N.

(E) Schematic diagram of human Ulk4 with wild type and mutated sequences of Stk36 sites, SUMOylation site and SIM motif shown.

(F) *in vitro* phosphorylation and SUMOylation of Ulk4. GST-fusion proteins containing wild type or mutant Ulk4C fragments were incubated with Fg-Stk36-EE purified from HEK293T cells and recombinant CK1, followed by *in vitro* SUMOylation by incubating with recombinant SUMO1, E1 and E2.

(G, H) Western blot analysis of Ulk4 SUMOylation in HEK293T cells co-transfected with the indicated Fg-Stk36 and Ulk4-HA constructs.

(I) Western blot analysis of Ulk4 SUMOylation in NIH3T3 cells infected with Ulk4-WT-HA or Ulk4-KR-HA construct and treated with or without Shh-N.

(J, K) Co-IP experiments to show Ulk4 self-association promoted by SUMO/SIM interaction. HEK293T cells were transfected with the indicated Ulk4 constructs, followed by immunoprecipitation and western blot analysis with the indicated antibodies.

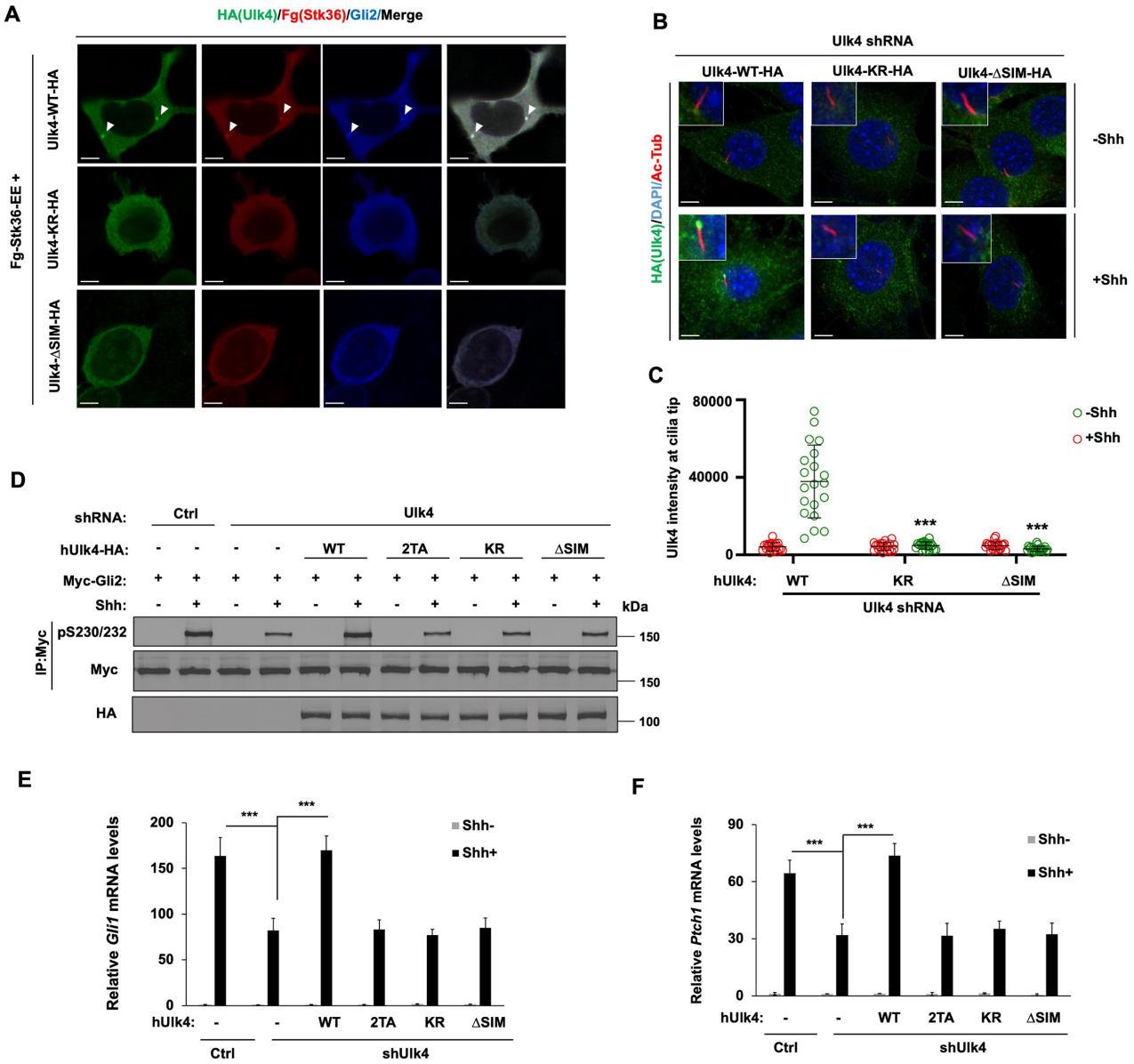

Fig. 5. SUMOylation promotes Ulk4 condensation, ciliary tip accumulation, and pathway activation dependent on SIM

(A) Representative images of immunostaining of HEK293T cells co-transfected with Fg-Stk36-EE and Ulk4-WT-HA, Ulk4-KR-HA or Ulk4-ΔSIM-HA constructs. Arrowheads indicate Ulk4 (green in A), Stk36 (red in A), or Gli2 (blue in A) puncta.

(B-C) Representative images of immunostaining (B) and quantification (C) of ciliary tip localized Ulk4-HA (green in B) in NIH3T3 cells infected with Ulk4 shRNA and the indicated human Ulk4 lentivirus in the presence or absence of Shh-N. Primary cilia were marked by acetylated tubulin (Ac-tub) staining (red in A) and nuclei by DAPI (Blue in A).

(D) Western blot analysis of Myc-Gli2 phosphorylation on S230/S232 in NIH3T3 cells expressing the control (Ctrl) or Ulk4 shRNA and the indicated Ulk4 lentiviral constructs and treated with or without Shh-N.

(E-F) Relative *Gli1* (E) and *Ptch1* (F) mRNA levels in NIH3T3 cells expressing the control (Ctrl) or Ulk4 shRNA and the indicated Ulk4 lentiviral constructs and treated with or without Shh-N.

The intensity of ciliary localized wild type and mutant Ulk4-HA was measured by Image J. 20 cells were randomly selected from each experimental group for quantification. Data are mean ± SD from three independent experiments. ***$p < 0.001$ (Student's t test).

Scale bars in A and B are 6 μm and 5 μm, respectively.

Zhou_Fig. 6

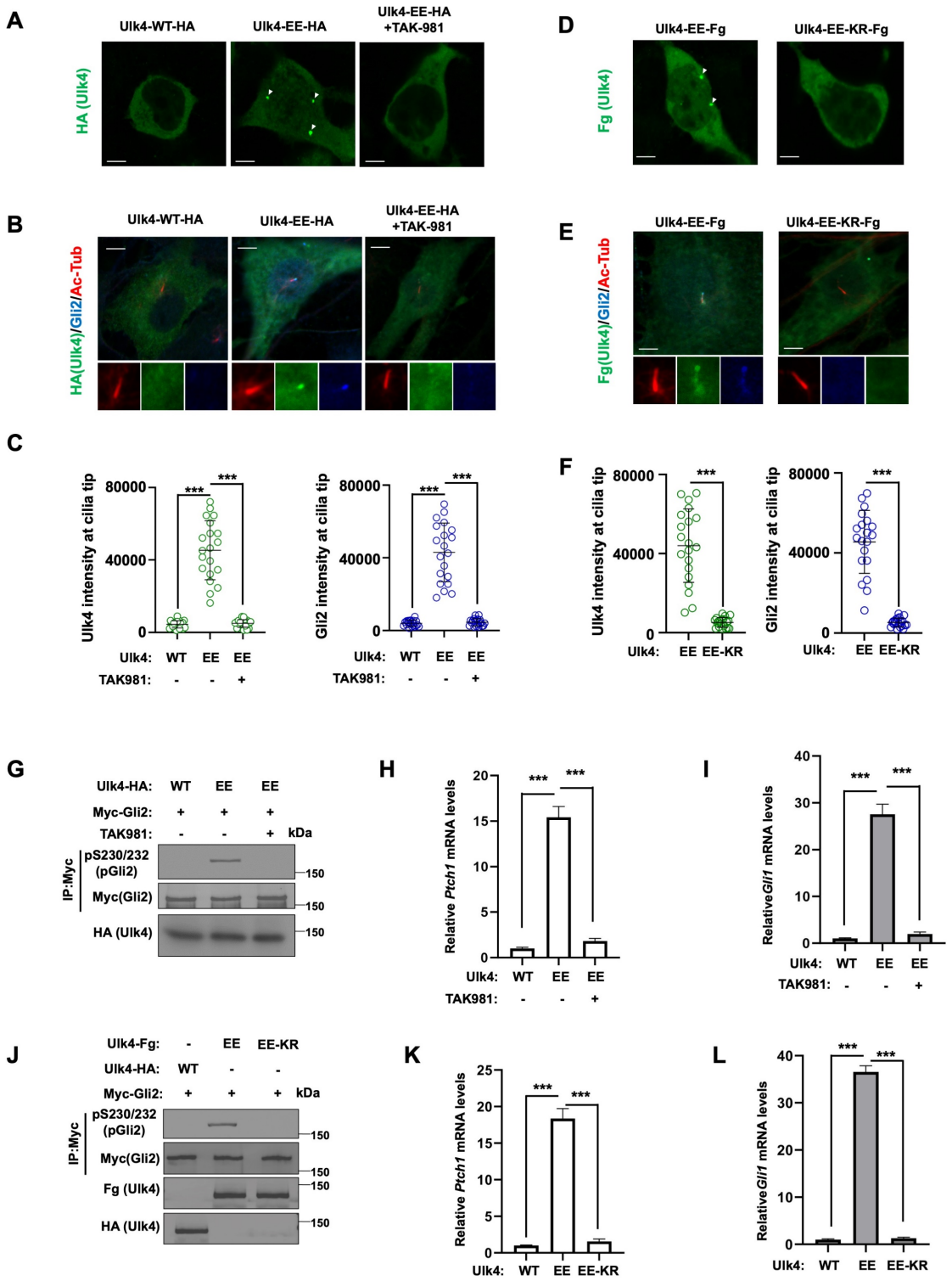
A
Ulk4-WT-HA
Ulk4-EE-HA
Ulk4-EE-HA +TAK-981
HA (Ulk4)
B
Ulk4-WT-HA
Ulk4-EE-HA
Ulk4-EE-HA +TAK-981
HA(Ulk4)/Gli2/Ac-Tub
C
Ulk4 intensity at cilia tip
Gli2 intensity at cilia tip
80000
40000
0
***
Ulk4: WT EE EE
TAK981: - - +
D
Ulk4-EE-Fg
Ulk4-EE-KR-Fg
Fg (Ulk4)
E
Ulk4-EE-Fg
Ulk4-EE-KR-Fg
Fg(Ulk4)/Gli2/Ac-Tub
F
Ulk4 intensity at cilia tip
Gli2 intensity at cilia tip
Ulk4: EE EE-KR
G
Ulk4-HA: WT EE EE
Myc-Gli2: + + +
TAK981: - - +
kDa
IP:Myc
pS230/232 (pGli2)
Myc(Gli2)
HA (Ulk4)
150
H
Relative Ptch1 mRNA levels
Ulk4: WT EE EE
TAK981: - - +
I
Relative Gli1 mRNA levels
Ulk4: WT EE EE
TAK981: - - +
J
Ulk4-Fg: - EE EE-KR
Ulk4-HA: WT - -
Myc-Gli2: + + +
kDa
IP:Myc
pS230/232 (pGli2)
Myc(Gli2)
Fg (Ulk4)
HA (Ulk4)
150
K
Relative Ptch1 mRNA levels
Ulk4: WT EE EE-KR
L
Relative Gli1 mRNA levels
Ulk4: WT EE EE-KR

Fig. 6. Ulk4-EE exhibits constitutive Hh pathway activity dependent on its SUMOylation

(A) Representative images of immunostaining of HEK293T cells transfected with the indicated Ulk4 expression constructs and treated with or without the SUMOylation inhibitor TAK981. Arrowheads indicate Ulk4 puncta. Scale bars are 6 μm.

(B, C) Representative images of immunostaining (B) and quantification (C) of ciliary tip localized Ulk4-WT-HA or Ulk4-EE-HA (green) and endogenous Gli2 (blue) in NIH3T3 cells treated with or without the SUMOylation inhibitor TAK981. Primary cilia were marked by acetylated tubulin (Ac-tub) staining (red). Scale bars are 5 μm.

(D) Representative images of immunostaining of HEK293T cells transfected with Ulk4-EE-Fg or Ulk4-EE-KR-Fg expression construct. Arrowheads indicate Ulk4 puncta. Scale bars are 6 μm.

(E, F) Representative images of immunostaining (E) and quantification (F) of ciliary tip localized Ulk4-Fg (green) and endogenous Gli2 (blue) in NIH3T3 cells infected with Ulk4-EE-Fg or Ulk4-EE-KR-Fg lentivirus. Primary cilia were marked by acetylated tubulin (Ac-tub) staining (red). Scale bars are 5 μm.

(G, J) Western blot analysis of Myc-Gli2 phosphorylation on S230/S232 in NIH3T3 cells co-infected with Myc-Gli2 and the indicated Ulk4 lentiviral constructs and treated with or without the SUMOylation inhibitor TAK981.

(H, I, K, L) Relative *Ptch1* (H, K) and *Gli1* (I, L) mRNA levels in NIH3T3 cells infected with the indicated Ulk4 lentiviral constructs and treated with or without the SUMOylation inhibitor TAK981.

The intensity of ciliary-localized wild type and mutant Ulk4-HA was measured by Image J. 20 cells were randomly selected from each experimental group for quantification. Data are mean ± SD from three independent experiments. ***$p < 0.001$ (Student's t test).

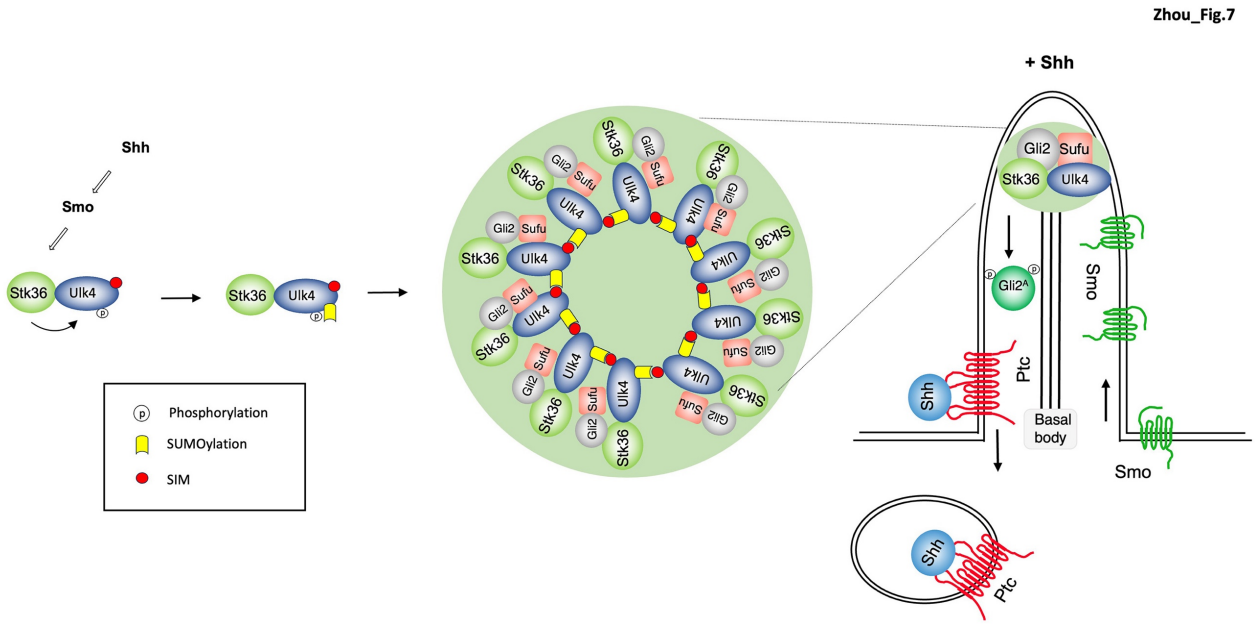

Fig. 7. Phosphorylation-induced SUMOylation promotes kinase/substrate condensation at ciliary tip

A working model in which Shh induces Ulk4/Stk36/Gli2/Sufu condensation at primary cilia. In response to Shh, Stk36 phosphorylates Ulk4 on T1021/T1023, which induces SUMOylation of Ulk4 on K1030. Subsequently, SUMO/SIM interaction drives the formation of Ulk4 condensates at ciliary tip that recruit Stk36, Gli2, and Sufu.

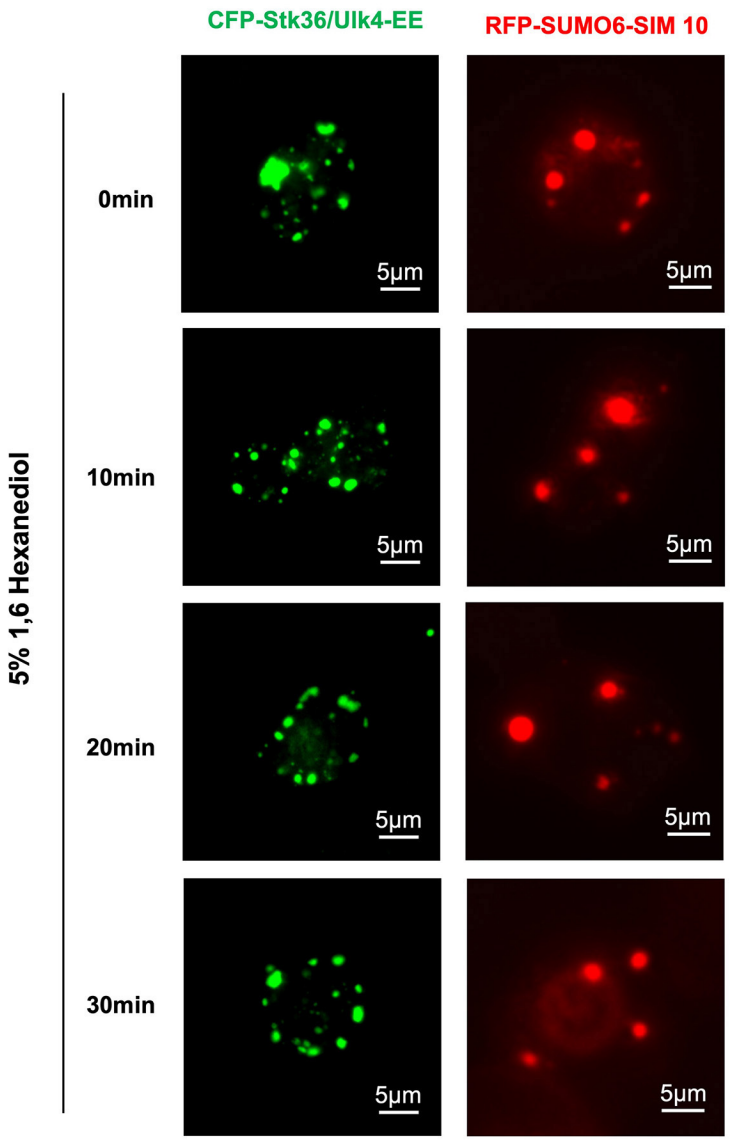

Fig. S1. Stk36/Ulk4 condensates are resistant to 1, 6-hexanediol

Representative images of HEK293T cells expressing the indicated constructs before and after treatment with 5% 1, 6-hexanediol for 10, 20, and 30 minutes.

Scale bars are 5 μm.

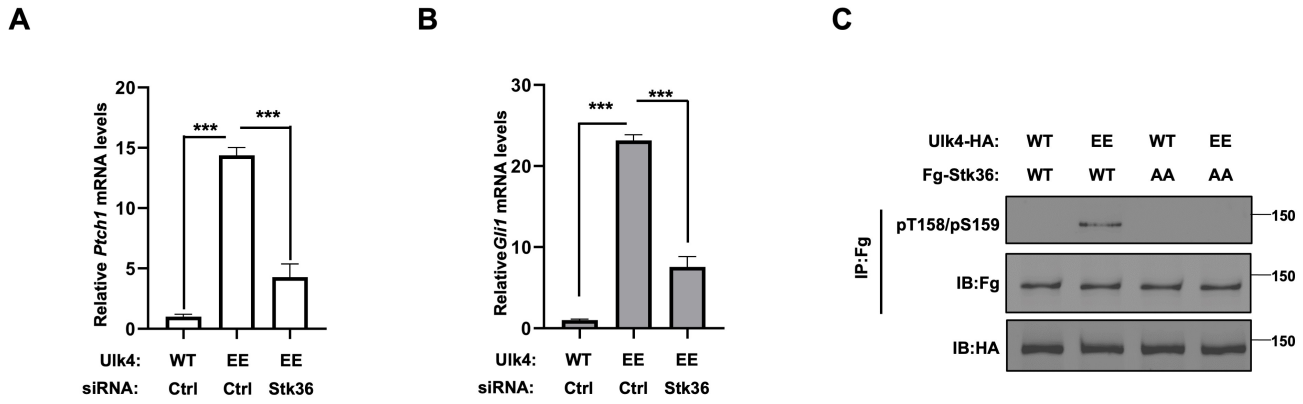

Fig. S2. The constitutive pathway activity of Ulk4-EE depends on Stk36

(A, B) Relative *Ptch1* (A) and *Gli1* (B) mRNA levels in NIH3T3 cells infected with the indicated Ulk4 lentiviral constructs and treated with control (Ctrl) or Stk36 siRNA.

(C) Western blot analysis of Stk36 phosphorylation on pT158/pS159 in NIH3T3 cells co-infected with the indicated Ulk4 and Stk36 lentiviral constructs.